Japanese Journal of Applied Physics

REGULAR PAPER

Brillouin scattering of multiferroic $BiFeO_3$

Japanese Journal of Applied Physics **62**, SM1014 (2023) **REGULAR PAPER**
https://doi.org/**10.35848/1347-4065/ace5b8**

Brillouin scattering of multiferroic $BiFeO_3$

Hiromu Ishida[1*], Eiichi Oishi[2], Yasuhiro Fujii[1], Akitoshi Koreeda[1], Takuya Satoh[3], and Toshimitsu Ito[4]

[1]*Department of Physical Sciences, College of Science and Engineering, Ritsumeikan University, Kusatsu, Shiga 525-8577, Japan*
[2]*Research Organization of Science and Technology, Ritsumeikan University, Kusatsu, Shiga 525-8577, Japan*
[3]*Department of Physics, Tokyo Institute of Technology, Meguro-ku, Tokyo 152-8551, Japan*
[4]*National Institute of Advanced Industrial Science and Technology, Tsukuba, Ibaraki 305-8565, Japan*

[*]E-mail: ishida.h22@kore-lab.org

Received June 2, 2023; revised July 6, 2023; accepted July 9, 2023; published online August 1, 2023

We performed Brillouin light scattering spectroscopy on a single crystal of $BiFeO_3$ (BFO) in the temperature range from 110 to 300 K and observed the Brillouin scattering from the LA and TA phonon modes, which were traveling along the *c*-axis. We determined the elastic constants for the LA mode (C_{33}) and TA mode (C_{44}) to be approximately 251 GPa and 38.7–44.2 GPa at 300 K, respectively. We observed splitting of the degenerate TA modes (corresponding to the elastic constant C_{44}), which is not expected for the TA modes traveling along the three-fold symmetry axis (the *c*-axis) of BFO. We also present the temperature dependences of the frequencies of the LA and TA modes, which include anomalies such as the LA mode softening and TA mode frequency drop at around 210 K.

1. Introduction

Recently, multiferroic materials that exhibit ferroelectric and antiferromagnetic properties have attracted a great deal of attention due to their potential for various applications, such as low power-consumption memory and spintronics devices.[1)] Among them, $BiFeO_3$ (BFO) has attracted special attention as the only compound that exhibits multiferroic properties even at RT due to its high Néel temperature (640 K)[2)] and Curie temperature (1100 K).[3)] The space group of its crystal structure is *R*3*c*, with spontaneous polarization along the *c*-axis, which is the $[111]_{pc}$ direction.[2,4)] BFO is also a G-type antiferromagnet with a spin cycloidal structure originating from the asymmetric Dzyaloshinsky–Moriya interactions.[5–10)] The propagation vectors of the spin cycloidal structure have equivalent directions that differ by 120 degrees, i.e. orienting to the pseudocubic $[10\bar{1}]_{pc}$, $[\bar{1}10]_{pc}$, $[0\bar{1}1]_{pc}$ directions and there are three orientations of the magnetic domains.[8)] Due to this characteristic crystal structure, in addition to the phonons and magnons, there are also electromagnons[11)] that originate from spin-lattice coupling.[12,13)]

Light scattering experiments in BFO have been actively conducted in order to understand the characteristic structures and dynamics of the phonons and magnons.[14–19)] Among them, there are many reports on Raman scattering occurring in the relatively HF region, namely, above ~10 cm^{-1} or 0.3 THz, where the optical phonons and magnons associated with the dielectric and magnetic ordering have been observed.[20–26)] However, there are few reports on Brillouin scattering in the sub-100 GHz frequency region, where the acoustic phonons and magnons are expected to be observed. The acoustic phonons in BFO have been observed by using pump-probe spectroscopy[27,28)] and pulse echo spectroscopy[29)] in polycrystalline samples, but there is no direct observation of the Brillouin light scattering in single crystals of BFO to the best of our knowledge. In this study, we report on the observation of the Brillouin light scattering in a single crystal of BFO and investigate the temperature dependence of the frequencies of the LA and TA phonon modes in the temperature range from 110 to 300 K.

2. Experimental methods

The sample used was identical to the one employed in previous study.[16)] It was a single crystal of BFO fabricated by the laser diode floating zone method,[30)] with a polished surface normal to the crystalline *c*-axis, i.e. the [111] direction of the cubic perovskite phase ($[111]_{pc}$), which is the ferroelectric polarization direction, as was confirmed experimentally.[31)] The sample was a circular plate with a diameter of 5 mm and a thickness of 0.2 mm. The refractive index of the sample at the wavelength of 532 nm was determined to be 2.9 from the reflectivity measurement and Fresnel's formula.

Figure 1 shows a schematic of the optical system used to observe Brillouin scattering. A linearly polarized single longitudinal mode Nd:YAG laser (Oxxius, LCX-532S-300) with a wavelength of 532 nm, which is longer than the absorption edge[32)] of the BFO, was focused on the sample surface by a 150 mm focal lens with an incident intensity of 15 mW. The diameter of the focused spot on the sample surface was approximately 100 μm. The heating of the sample due to the laser irradiation was estimated to be approximately 3 K from the laser power dependence of the Brillouin shifts. By the observation with polarization microscope, we selected a single ferroelectric domain with the spontaneous electric polarization oriented to the sample normal.[16,31)] The area of the selected ferroelectric domain was approximately 17 mm^2, which was sufficiently larger than the focused spot of the illuminating laser. The spectrometer employed was a tandem Fabry–Perot interferometer (JRS Scientific Instruments, TFP-1),[33)] with a HF resolution and high contrast owing to the connection of two sets of planar Fabry–Perot mirrors in series and bouncing the transmitted light back three times. The free spectral range of the Fabry–Perot was 100 GHz, and the average number was 2000 times. The backscattered light was polarization-analyzed and collected into the spectrometer. The sample was tilted by approximately 8 degrees from normal incidence to suppress elastic scattering during the measurement. Taking

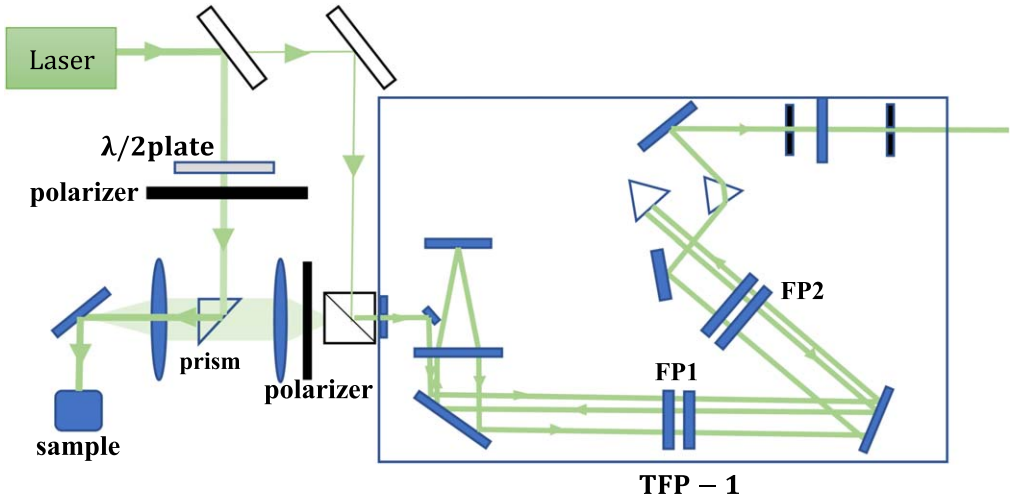

Fig. 1. Optical setup for Brillouin scattering. FP represents Fabry–Perot interferometer.

into account the refractive index of BFO ($n = 2.9$), the phonon propagation direction was estimated to deviate by 2.8 degrees from the c-axis. To check the effect of the deviation of the phonon propagation direction from the c-axis, we set the sample just normal to the incident beam, but we did not find any quantitative difference in the spectrum except the significant increase of the intensity of the elastic Rayleigh scattering peak. Thus, we concluded that we effectively observed phonons traveling along the c-axis of BFO (along the $[111]_{pc}$ direction). The light polarization conditions of the incident and scattered lights were HH (parallel Nicols) and HV (crossed Nicols), where the H and V represent horizontal and vertical polarizations, respectively, with respect to the laboratory coordinates. We verified that the H direction was parallel to the crystalline $[10\bar{1}]_{pc}$ direction from the measurements of the polarization-angle resolved Raman spectroscopy on the magnons in the same sample.[30] The heating and cooling stage was Linkam 10002L manufactured by Japan High Tech, and the temperature was changed from 110 to 300 K by heating.

3. Results and discussion

Figure 2 shows the Brillouin spectra of the BFO single crystal observed at 110 K in HH and HV configurations. In the HH spectrum, there are three peaks at approximately 60, 33, and 24 GHz. Among these peaks, the 33 GHz peak, labeled as "W", was identified as the Brillouin scattering from the window material (fused silica). In the HV spectrum, there is only one peak at approximately 26 GHz. The sharp peak at the center is the spectrum of the incident laser, and the discontinuity appearing around 5 GHz is due to the shutter operation for the intense Rayleigh scattering not to enter the spectrometer. For backscattering geometry, the frequency shift of the Brillouin scattering is given by

$$\nu_B = \pm\frac{2nv}{\lambda_l}, \text{ with } v = \sqrt{\frac{C}{\rho}}, \tag{1}$$

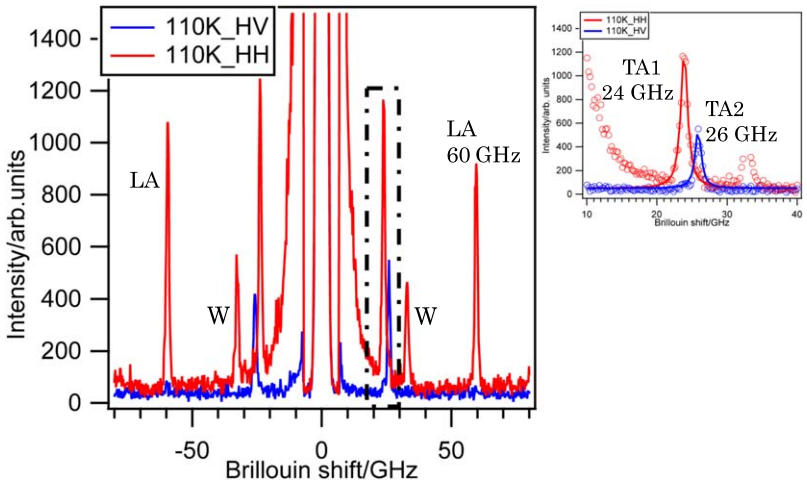

Fig. 2. Brillouin spectra of the BFO single crystal observed at 110 K in HH and HV configurations. The inset is a magnifield spectrum around 25 GHz part (in the dotted line). In the HH spectrum, there are three peaks at approximately 60, 33, and 24 GHz. Among these peaks, the 33 GHz peak, labeled as "W", was identified as the Brillouin scattering from the window material (fused silica). In the HV spectrum, there is only one peak at approximately 26 GHz.

where λ_1, n, v, C, and ρ are the wavelength of the laser, refractive index, speed of sound (TA or LA phonons), elastic constant, and density, respectively. Thus, by observing Brillouin scattering, the corresponding sound velocity can be obtained, and the elastic constants can be determined from an experimental standpoint.

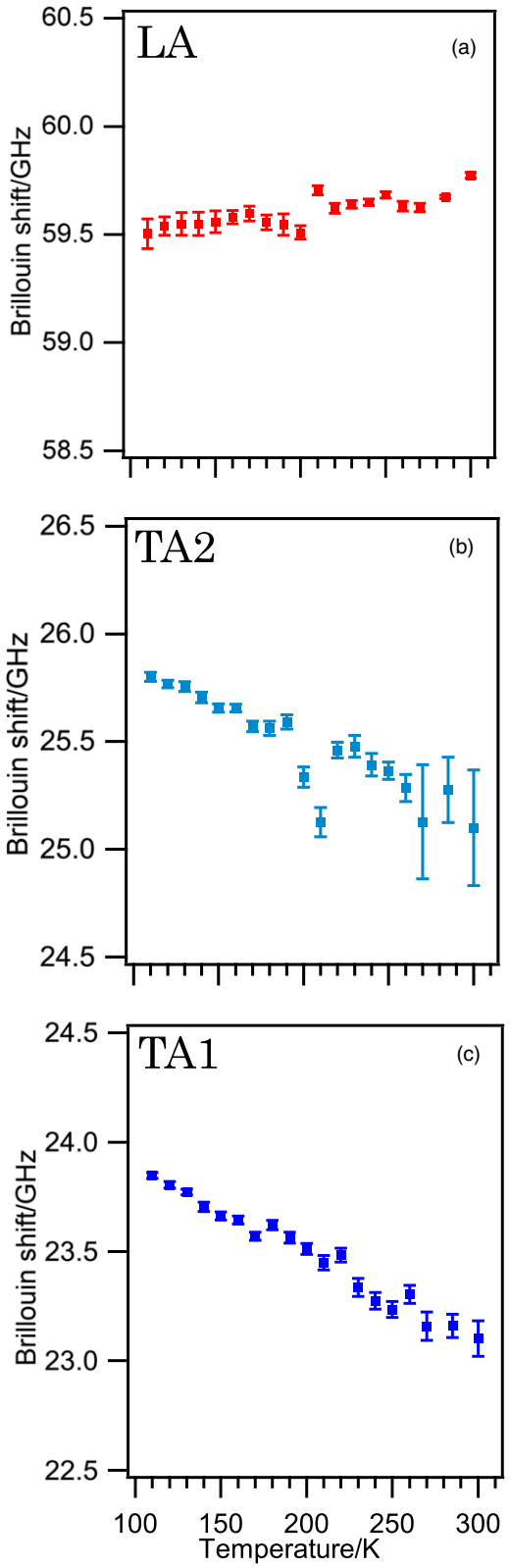

Fig. 3. The temperature dependence of the frequency shifts of the observed acoustic phonons: (a) LA, (b) TA2, and (c) TA1.

For the acoustic phonons traveling along the c-axis of BFO (along the $[111]_{pc}$ direction), we expect to observe an LA and a TA modes in the HH configuration and a TA mode in the HV configuration.[34,35)] From the HH spectrum observed at 300 K, we obtained the Brillouin shifts of 59.8 and 23.5 GHz. From Eq. (1), these yield velocities of 5490 m s^{-1} and 2160 m s^{-1}, respectively, which are comparable to those reported by Lejman et al. for the LA and TA sound velocities of a polycrystalline BFO at RT.[27)] Thus, we assign the Brillouin peaks appearing in the HH spectra to be the LA and TA phonon modes, and we obtain that $v_{LA} = 5490$ m s^{-1} and $v_{TA1} = 2160$ m s^{-1} at RT. For the LA mode traveling along the c-axis of BFO, the corresponding elastic constant is C_{33}.[35)] From the relation

$$\rho v_{LA}^2 = C_{33}, \tag{2}$$

we obtain that $C_{33} = 251$ GPa, adopting the density of BFO to be $\rho = 8.34$ g cm^{-3}.[28)] The obtained value is substantially larger than the previously reported values of $C_{33} \approx$ 160–180 GPa[36,37)] which might be due to the difference in the sample qualities of the BFO single crystals.

According to elasticity theory,[35)] all the TA waves traveling along the $[111]_{pc}$, which is a three-fold symmetry axis, should be degenerated in frequency[34,35,38)] and the corresponding elastic constant should be equal to C_{44}, i.e. the elastic nature in a plane normal to the three-fold symmetry axis is isotropic. However, in our experiment, the frequency shifts of TA1 (observed in the HH spectra) and TA2 (observed in the HV spectra) are different by about 2 GHz, which is not compatible with the expected elastic isotropy for the three-fold symmetry. One of the possible reasons for this frequency difference may be that the phonon propagation direction was deviated by about 2.8 degrees from the c-axis. However, as we mentioned in Sect. 2, we did not detect any quantitative difference in frequency shifts of the LA, TA1, and TA2 in the spectra within the experimental error (≈0.1 GHz) even when we set the sample just normal to the incident beam. Thus, the slight deviation of the phonon propagation direction from the c-axis is ruled out for the explanation of the observed frequency difference between TA1 and TA2.

Another possibility taking into account the multiferroic nature of BFO is that there may be non-negligible interaction between the phonons and magnons. Since BFO is a G-type antiferromagnet with a spin-cycloidal structure originating from the asymmetric Dzyaloshinskii–Moriya interactions,[5–10)] the propagation vectors of the spin-cycloidal structure have equivalent directions that differ by 120 degrees in the $(111)_{pc}$ plane, and there are three orientations of the magnetic domains. Thus, if there is an interaction between the lattice (elastic property) and magnetism (spin cycloids), the combined system can no more be isotropic in the $(111)_{pc}$ plane. To verify this hypothesis, it is necessary to conduct polarization angle-resolved light scattering measurements, rotating the polarization plane of the incident light around the c-axis of the BFO sample.

Since the frequency shifts of the TA1 and TA2 modes at RT were 23.5 GHz and 25.1 GHz, respectively, the sound velocities are estimated to be $v_{TA1} = 2160$ m s^{-1} and $v_{TA2} = 2300$ m s^{-1}. From the relation

$$\rho v_{TA}^2 = C_{44}, \quad (3)$$

we estimate that $C_{44} \approx 38.7-44.2$GPa at RT, neglecting the slight difference in the frequency shifts of TA1 and TA2. This value is in good agreement with reported values of $C_{44} \approx 30$–40 GPa.[36,37)]

The temperature dependence of the frequency shifts of the observed acoustic phonons is plotted in Figs. 3(a)–3(c), where we see that the LA mode becomes softer with decreasing temperature below RT, while both of the TA modes become harder. The relatively large error bars for the TA2 at high temperatures are due to the weak signal intensity resulting from the partial absorption of 532 nm light at around 300 K; at lower temperatures, the signal intensity increases because the absorption edge shifts to the shorter wavelength on cooling. While the hardening of phonons on cooling is an ordinary behavior,[39,40)] the softening of the LA mode on cooling is somewhat unusual, which is not covered in the previous measurements conducted at higher temperatures.[27)] The temperature dependences of n and/or ρ can be the origin of this apparent softening (frequency decrease), but it is not compatible with the hardening of the TA modes, where the identical n and/or ρ values are relevant. At this stage, we have no idea about this unusual phonon behavior of the LA mode.

In Fig. 3(b), an anomalous behavior is observed at around 210 K for the TA2 mode; there is a clear frequency drop at around 210 K. In the previous studies on the Raman spectroscopy of the magnons in BFO, a frequency drop of a magnon mode at a temperature around 200 K was reported, and it was proposed that the magnon anomaly should be related to the spin reorientation,[41,42)] which is a magnetic phase transition. Our observation of the phonon anomaly of the TA2 mode at around 210 K may be caused by the proposed spin reorientation and spin-lattice interaction because of the coincidence of the temperature and the unexpected phonon anisotropy that might be related to the magnetic order, which we have described above. Although a slight frequency jump is also seen in the LA frequency at 210 K, the change is not sufficiently large compared to the experimental error of 0.1 GHz that we discuss whether the LA mode is also related to such a spin-lattice interaction.

4. Conclusions

Brillouin scattering observations on a single crystal of BFO have revealed acoustic phonon properties in the temperature range from 110 to 300 K. The elastic constant relevant for the LA mode traveling along the c-axis, C_{33}, was determined to be 251 GPa at RT. C_{33} was found to become slightly softer with decreasing temperature. The TA modes (TA1 and TA2) were found to have slightly different elastic constants; $C_{44} \approx 38.7-44.2$ GPa, which might be related to the anisotropy induced by the spin-lattice coupling. The TA2 mode showed an anomalous behavior at 210 K, which might be due to the proposed spin reorientation and spin-lattice interaction.[12,41,42)]

In the future, we would like to perform polarization angle-resolved measurements to investigate the relation with the cycloidal structure of spins. In addition, it has been reported in Raman scattering experiments that the magnon behavior changes between right and left circularly polarized light,[26)] and we believe that circularly polarized Brillouin spectroscopy may clarify the cause of the anomalous TA2 behavior. The laser spot size in this experiment was 100 μm, while the antiferromagnetic domain of the sample used in this study was measured to be only a few μm.[43)] Since it is necessary to discuss the behavior within single antiferromagnetic domain, we would like to conduct microscopic Brillouin spectroscopy measurements in a microscope system. In addition, it is necessary to extend the temperature range of the present measurement to lower temperatures, viz., 4–300 K and to confirm whether the anomaly reported at 50 K[44)] behaves in the same way. Since there are few reports on Brillouin scattering in BFO, the behavior of the acoustic phonon modes observed in this study should be discussed further in the future.

Acknowledgments

This study was supported by JSPS KAKENHI Grant No. JP19H05618, JP21H01018.

ORCID iDs

Eiichi Oishi https://orcid.org/0000-0002-2961-5952
Yasuhiro Fujii https://orcid.org/0000-0002-9522-6103
Akitoshi Koreeda https://orcid.org/0000-0002-3063-5563
Takuya Satoh https://orcid.org/0000-0001-6270-0617
Toshimitsu Ito https://orcid.org/0000-0003-2094-2807

1) K. Wang, J. M. Liu, and Z. Ren, Adv. Phys. **58**, 321 (2009).
2) J. Moreau, C. Michel, R. Gerson, and W. James, J. Phys. Chem. Solids **32**, 1315 (1971).
3) R. T. Smith, G. D. Achenbach, R. Gerson, and W. J. James, J. Appl. Phys. **39**, 70 (1968).
4) F. Kubel and H. Schmid, Acta Crystallogr., Sect. B **46**, 698 (1990).
5) M. Ramazanoglu, W. Ratcliff, Y. J. Choi, S. Lee, S.-W. Cheong, and V. Kiryukhin, Phys. Rev. B **83**, 174434 (2011).
6) H. J. ZhaO, P. Chen, S. Prosandeev, S. Artyukhin, and L. Bellaiche, Nat. Mater. **20**, 341 (2021).
7) I. Sosnowska, T. P. Neumaier, and E. Steichele, J. Phys. C: Solid State Phys. **15**, 4835 (1982).
8) D. Lebeugle, D. Colson, A. Forget, M. Viret, A. M. Bataille, and A. Gukasov, Phys. Rev. Lett. **100**, 227602 (2008).
9) S. Lee, W. Ratciff, S.-W. Cheong, and V. Kiryukhin, Appl. Phys. Lett. **92**, 192906 (2008).
10) J. Herrero-Albillos, G. Catalan, J. A. Rodriguez-Velamazan, M. Viret, D. Colson, and J. F. Scott, J. Phys.: Condens. Matter **22**, 256001 (2010).
11) D. Talbayev, S. A. Trugman, S. Lee, H. T. Yi, S.-W. Cheong, and A. J. Taylor, Phys. Rev. B **83**, 094403 (2011).
12) M. K. Singh, R. S. Katiyar, and J. F. Scott, J. Phys.: Condens. Matter **20**, 252203 (2008).
13) U. Nagel, R. S. Fishman, T. Katuwal, H. Engelkamp, D. Talbayev, H. T. Yi, S. W. Cheong, and T. Rõõm, Phys. Rev. Lett. **110**, 257201 (2013).
14) S. Skiadopoulou, V. Goian, C. Kadlec, F. Kadlec, X. F. Bai, I. C. Infante, B. Dkhil, C. Adamo, D. G. Schlom, and S. Kamba, Phys. Rev. B **91**, 174108 (2015).
15) E. Matsubara, T. Mochizuki, M. Nagai, and M. Ashida, Phys. Rev. B **94**, 054426 (2016).
16) P. Khan, M. Kanamaru, K. Matsumoto, T. Ito, and T. Satoh, Phys. Rev. B **101**, 134413 (2020).
17) R. Palai, H. Schmid, J. F. Scott, and R. S. Katiyar, Phys. Rev. B **81**, 064110 (2010).
18) J. Hlinka, J. Pokorny, S. Karimi, and I. M. Reaney, Phys. Rev. B **83**, 020101 (2011).
19) M. Cazayous, Y. Gallais, A. Sacuto, R. de Sousa, D. Lebeugle, and D. Colson, Phys. Rev. Lett. **101**, 037601 (2008).
20) R. Haumont, J. Kreisel, and P. Bouvier, Phese Transit. **79**, 1043 (2006).
21) D. Kothari, V. Raghavendra Reddy, V. G. Sathe, A. Gupta, A. Banerjee, and A. M. Awasthi, J. Magn. Magn. Mater. **320**, 548 (2008).
22) P. Rovillain, M. Cazayous, Y. Gallais, A. Sacuto, R. P. S. M. Lobo, D. Lebeugle, and D. Colson, Phys. Rev. B **79**, 180411 (2009).

23) P. Rovillain, M. Cazayous, A. Sacuto, D. Lebeugle, and D. Colson, J. Magn. Magn. Mater. **321**, 1699 (2009).
24) Y. Yang, L. G. Bai, K. Zhu, Y. L. Liu, S. Jiang, J. Liu, J. Chen, and X. R. Xing, J. Phys.: Condens. Matter **21**, 385901 (2009).
25) T. Shimizu, T. Era, H. Taniguchi, D. Fu, T. Taniyama, and M. Itoh, Ferroelectrics **403**, 187 (2010).
26) E. Oishi, Y. Fujii, A. Koreeda, T. Satoh, and T. Ito, Jpn. J. Appl. Phys. **61**, SN1021 (2022).
27) M. Lejman, C. Paillard, V. Juvé, G. Vaudel, N. Guiblin, L. Bellaiche, M. Viret, V. E. Gusev, B. Dkhil, and P. Ruello, Phys. Rev. B **99**, 104103 (2019).
28) P. Ruello, T. Pezeril, S. Avanesyan, G. Vaudel, V. Gusev, I. C. Infante, and B. Dkhil, Appl. Phys. Lett. **100**, 212906 (2012).
29) E. P. Smirnova, A. Sotnikov, S. Ktitorov, N. Zaitseva, H. Schmidt, and M. Weihnacht, Eur. Phys. J. B **83**, 39 (2011).
30) T. Ito et al., Cryst. Growth Des. **11**, 5139 (2011).
31) N. Sono, Y. Kinoshita, N. Kida, T. Ito, H. Okamoto, and T. Miyamoto, J. Phys. Soc. Jpn. **90**, 033703 (2021).
32) K. Li, W. Zhang, K. Guo, R. Cui, C. Deng, and X. Wang, Mater. Res. Express **9**, 036402 (2022).
33) J. R. Sandercock, J. Phys. E **9**, 566 (1976).
34) W. Hayes and R. Loudon, *Scattering of Light by Crystals* (Wiley-Interscience, Canada, 2009) p. 337.
35) R. Vacher and L. Boyer, Phys. Rev. B **6**, 639 (1972).
36) E. Borissenko, M. Goffinet, A. Bosak, P. Rovillain, M. Cazayous, D. Colson, P. Ghosez, and M. Krisch, J. Phys.: Condens. Matter **25**, 102201 (2013).
37) P. Hemme et al., Appl. Phys. Lett. **118**, 062902 (2021).
38) H. S. Lim, J. D. Huang, V. L. Zhang, M. H. Kuok, and S. C. Ng, J. Appl. Phys. **93**, 9703 (2003).
39) E. Oishi, Y. Fujii, A. Koreeda, A. Nagakubo, and H. Ogi, Jpn. J. Appl. Phys. **56**, 10PB06 (2017).
40) S. Ohno, T. Sonehara, E. Tatsu, A. Koreeda, and S. Saikan, Phys. Rev. B **95**, 224301 (2017).
41) M. K. Singh, S. Dussan, W. Prellier, and R. S. Katiyar, J. Magn. Magn. Mater. **321**, 1706 (2009).
42) J. F. Scott, J. Magn. Magn. Mater. **321**, 1689 (2009).
43) E. Oishi, Y. Fujii, A. Koreeda, T. Satoh, and T. Ito, in preparation.
44) S. A. T. Redfern, C. Wang, J. W. Hong, G. Catalan, and J. F. Scott, J. Phys.: Condens. Matter **20**, 452205 (2008).